Journal of Fluorescence
https://doi.org/10.1007/s10895-025-04235-9

RESEARCH

Study of DFT, Synthesis, and Nonlinear Optical Properties of a Schiff Base Compound

Ghufran A. Mirdan[1] · Qusay M. A. Hassan[2] · Mouayed Y. Kadhum[3] · C. A. Emshary[2] · Kawkab Ali Hussein[3] · H. A. Sultan[2] · Sadiq M. H. Ismael[3] · Hasanain A. Abdullmajed[1]

Received: 20 December 2024 / Accepted: 27 February 2025

Abstract

A Schiff base (LS2) compound is synthesized via a reaction of a hot ethanolic solution of (3-ethoxy salcyaldehyde) and a hot ethanolic solution of amine(methyl-4-amino benzoate). The LS2 compound is characterized via ^{1}H and ^{13}C NMR spectra, Mass spectrum, and FT-IR spectrum. We observed multiple diffraction patterns of a cw 473 nm laser beam from the LS2 compound caused by spatial self-phase modulation (SSPM). The nonlinear refractive index (NLRI) of the LS2 compound is estimated at the high-power input of the laser beam and found equals to 5.387×10^{-7} cm^2/W. The Z-scan techniques are used to estimate the NLRI and found equals to 0.12×10^{-7} cm^2/W. The all-optical switching (AOS) effect can be seen when 473 nm is used as the controlling beam and 532 nm is used as the controlled beam.

Keywords Schiff base compound · Z-scan · Diffraction patterns

Introduction

During the past few years, we have been engaged in the study of newly synthesized organic materials [1–6] for the sake of possible use in different photonic applications. These materials should exhibit rapid response in extremely brief periods and possess substantial nonlinear refractive indexes (NLRIs) [7–12]. Among the techniques used in the estimation of these materials NLRIs, there are two important techniques viz., the diffraction patterns (DPs) and the Z-scan [13–16] under the irradiation with CW, low power, visible laser beams. The methods are accurate, fast, and simple. Each requires small number of apparatus and limited period of time.

Schiff base is an analogue of a ketone or aldehyde in which the carbon group (C = 0) has been replaced by an amine or azomethine group. Alarge number of shiff base complexes are characterized by an excellent catalytic activity in a variety of reactions at high temperature and in the presence of moisture. Schiff base and their metal complexes are increasing being used as catalysis in various biological systems dye and polymers. Due to its various properties viz. in medicine and pharmacy, biological, antifungal, biocidal, antiviral, antimalarial, and anticancer, Schiff base are studied extensively viz. applications in modern technologies, in synthesis and chemical analysis [17].

The nonlinear optical properties of Schiff base have been studied minorally such as their optoelectronic properties [18], nonlinear optical properties [19], third-order optical properties using the Z-scan method [20]. We have studies the Schiff base nonlinear optical properties extensively during the last four years via diffraction patterns and the Z-scan [21–25].

The purpose of the current work is to find a material that has higher nonlinear optical properties compared to currently known materials so that it can be used in optical devices. So in the present work a Schiff base compound was synthesized and characterized using ^{1}H and ^{13}C NMR spectroscopies, Mass spectrum and FTIR spectrum. In this study, the Schiff base compound's nonlinear optical (NLO) features were looked at by using diffraction patterns and a visible, low-power laser beam to figure out the nonlinear

✉ Qusay M. A. Hassan
qusayali64@yahoo.co.in

[1] Ministry of Education, General Directorate of Education, Basrah, Iraq

[2] Department of Physics, College of Education for Pure Sciences, University of Basrah, Basrah 61001, Iraq

[3] Department of Chemistry, College of Education for Pure Sciences, University of Basrah, Basrah 61001, Iraq

Published online: 08 March 2025

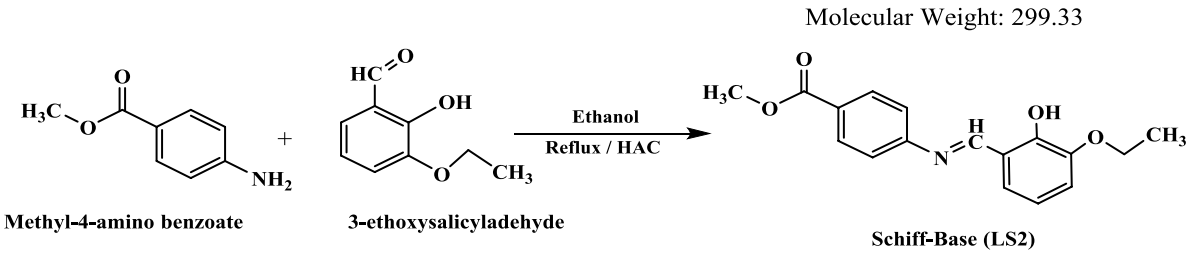

Fig. 1 Synthesis of LS2 compound

refractive index (NLRI). Two CW laser beams were used to test the all-optical switching (AOS).

Experimental

Materials and Methods

Merck and Aldrich obtained all chemicals and liquids, which were thereafter employed without further purification. The SHIMADZU FT-IR-8400S was utilized to capture infrared spectra on KBr discs. The Thermo Scientific 9100 was utilized to ascertain the melting points of diverse substances. The ^{1}H and ^{13}C-NMR spectra of the compounds were obtained in $CHCl_3$ at room temperature utilizing a Bruker 400 MHz spectrometer. The UV–visible spectrum was obtained utilizing ethanol as a solvent with the Shimadzu UV-1800 spectrophotometer. The mass spectrum was obtained via the E1 Technique with Agilent Technologies spectrometers calibrated to 70 eV. Thin layer chromatography (TLC) has been employed to assess the completion of processes.

Synthesis of Methyl (E)–4-((3-ethoxy-2-ydroxybenzylidene) amino) Benzoate (compound LS2)

Figure 1 depicts the Schiff-base (LS2) complex in a simplified format. A small quantity of glacial acetic acid was employed to react with a heated ethanolic solution of aldehyde (3-ethoxy salicylaldehyde) (0.9971 g, 0.006 mol) and a heated ethanolic solution of amine (methyl-4-amino benzoate) (0.9070 g, 0.006 mol) in ethanol to synthesize LS2. The liquid was cooled to room temperature following heating. The precipitate was dried, filtered, and recrystallized with pure ethanol. Orange color; yield: 89%; M.P 133–135 °C; FT-IR (ν cm^{-1}): 2980 (ν C-H aliphatic), 1708 (ν C=O), 1595 (ν C=N), 1570–1442 (ν C=C), 1278 (ν C-N); ^{1}H NMR ($CDCl_3$, 400 MHz; δ ppm) δ: 13.36 (s, 1H, OH), 8.62 (s, 1H, HC=N), 8.09–6.84(m, 7H, Ar–H), 4.13(s,3H, O-CH_2), 3.90(s,3H, O-CH_3), 1.5(s,3H, CH_3); ^{13}C NMR ($CDCl_3$,; δ ppm): 166.52 (C_2, C=O), 164.15(C_9, C=N), 152.07 (C_{11}, C–OH), 151.81 (C_{11}, C-OC_2H_5), 147.74 (C_6, C-N), 131.05–116.73($C_{4,5,7,8,13–15}$, C=C), 64.63(C_{16}, Ar–O-CH_2), 52.20(C_1, O-CH_3), 14.89(C_1, CH_3); MS: m/z: 299.1[M^+], UV–vis. in Ethanol, transitions: 220, 292 ($\pi \rightarrow \pi^*$) and 345 ($n \rightarrow \pi^*$)] cm^{-1}.

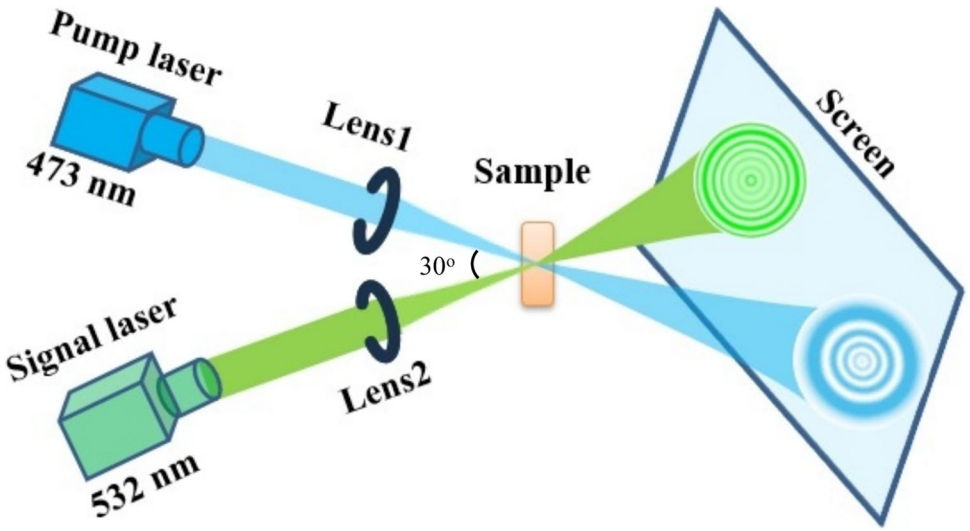

Fig. 2 Experimental set-up of all-optical switching

Table 1 The FT-IR spectra of the compound LS2

Band assignment	Wavenumber (cm^{-1})
νOH group	3450
νCH_3 Aromatic	3010
νCH_3 Aliphatic	2980
C = O Ester acid group	1708
ν(HC = N-) group of the azomethine	1595
νC = C conjugated	1570
νC-O group	1278

Experimental

To carry out the nonlinear index studies experiments, two solid state lasers emitting two CW beams of wavelengths 473 nm and 532 nm. Both lasers having spot sizes of 1.5 mm as each beams leaves the devices output coupler. A 5 cm focal length lens used to focus the first beam to a spot size of 19.235 µm used in the diffraction patterns and the Z-scan experiments, Two, 20 cm focal length, lenses used in the all-optical switching so that the spot sizes at each lens focus equals to 76.941 and 86.539 µm respectively. The experimental set-up of all-optical switching is displayed in Fig. 2. The DPs resulted was fall on two semitransparent screens viz. 30 × 30 cm and 60 × 60 cm for the DPs experiments and the all-optical switching respectively. To register the DPs a digital camera having an exposure time of (1/32) sec was used. In both CA Z-scan and OA Z-scan experiments the sample was moved the distance (-z) –(+ z) using a translational stage, passing through the lens focus (z = 0). The Rayleigh range of the two beams are $R_{z.473}$ and $R_{z.532}$ equals 2.356 and 2.763 mm.

Results

Chemistry

Schiff base LS2 molecules were made by reacting methyl-4-amino benzoate with the right aldehydes (3-ethoxy salicylaldehyde), as shown in Fig. 1. ^{1}H-NMR, ^{13}C-NMR, FT-IR, and mass spectra data helped us figure out the structures of the chemical we made. The LS2 compound's FTIR spectrum shows bands at 1708 cm^{-1}, which are caused by the ν(C = O) group. A band of absorption at 1595 cm^{-1} can be seen in the infrared readings of the LS2 compound. Assigned to the (C = N) stretching vibrations, which show that the azomethine band is forming. Furthermore, the lack of primary amine group stretching vibrations in the compound's spectra shows that Schiff base condensation took place, with the appearance of the κ(C = C) band between

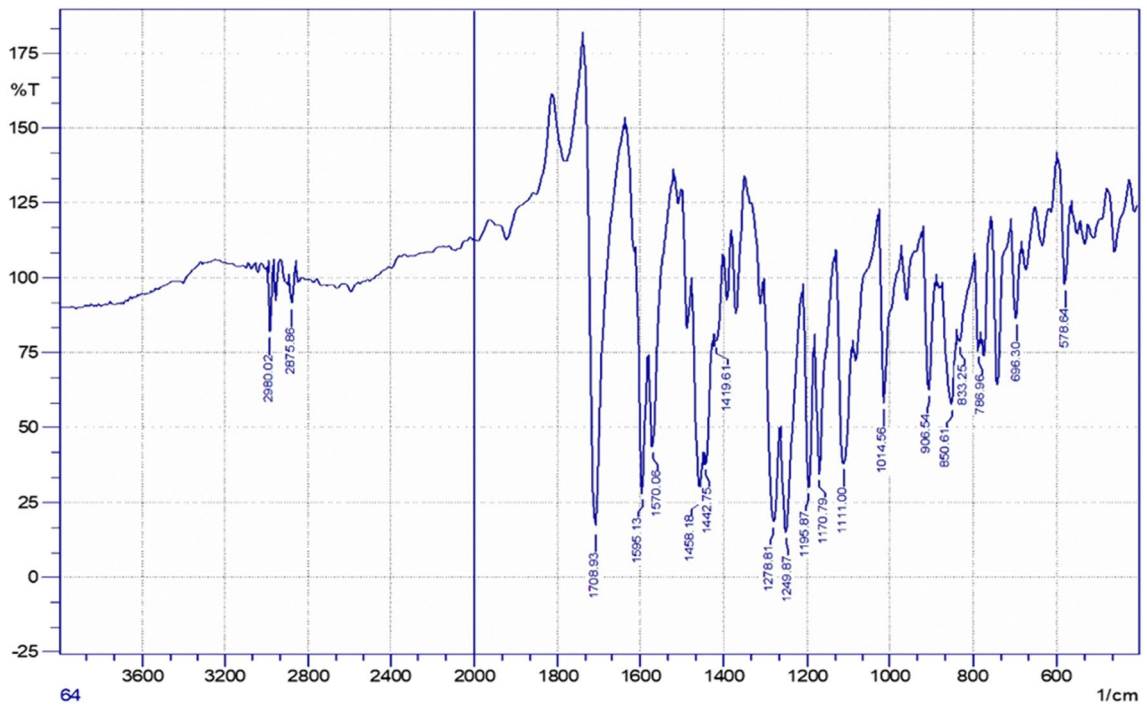

Fig. 3 FT-IR Spectrum of the LS2 compound

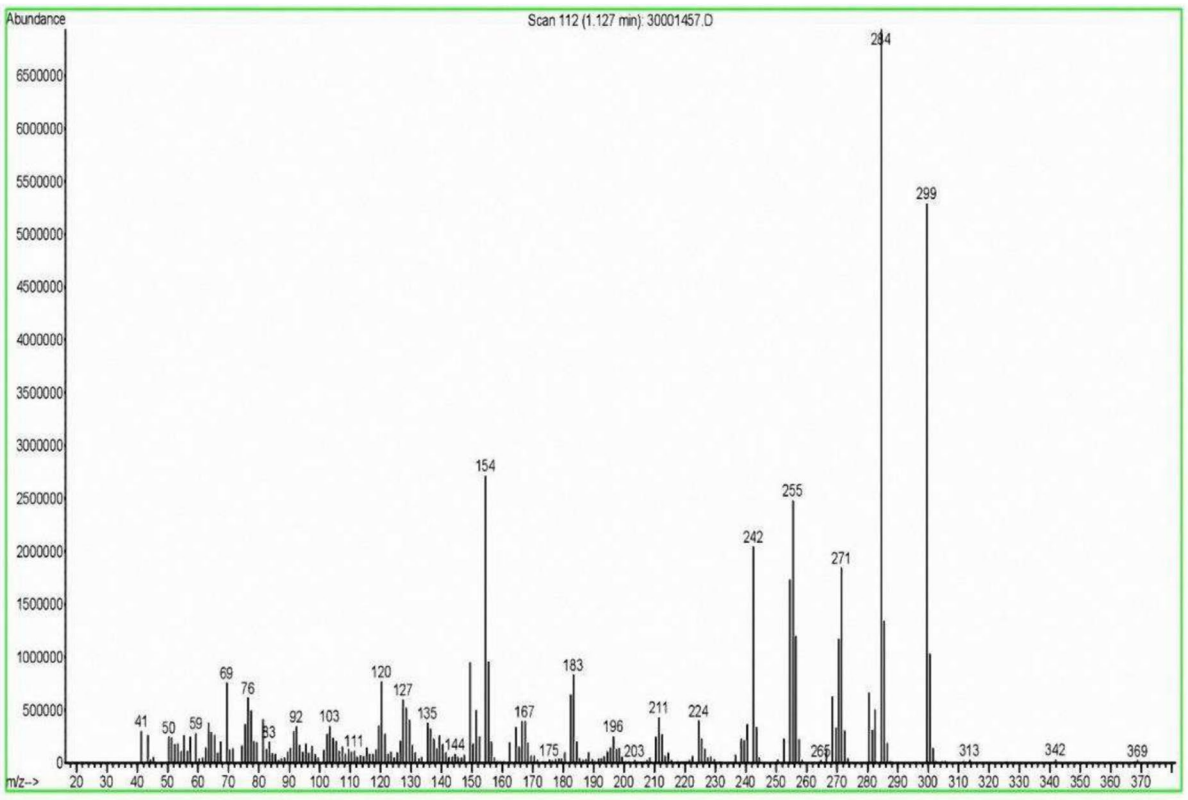

Fig. 4 Mass spectrum of the LS2 compound

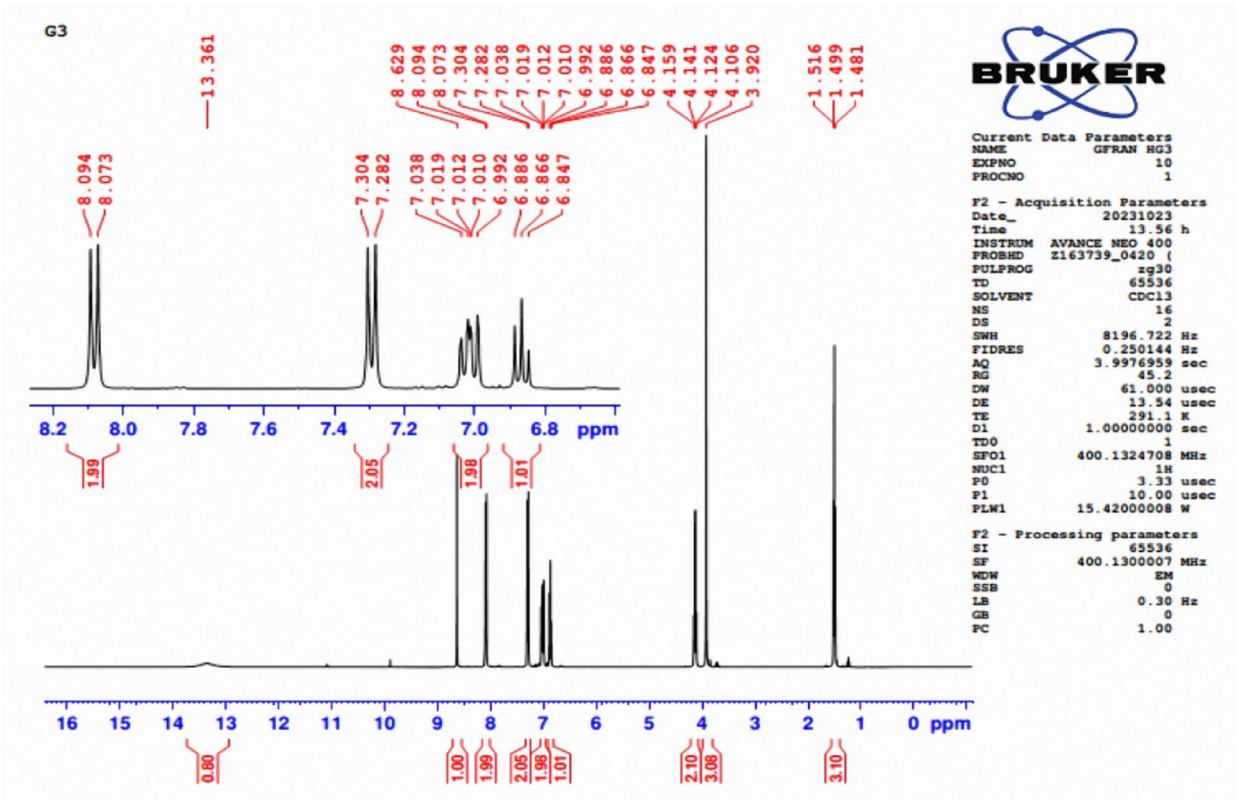

Fig. 5 [1]HNMR spectrum of the LS2 compound

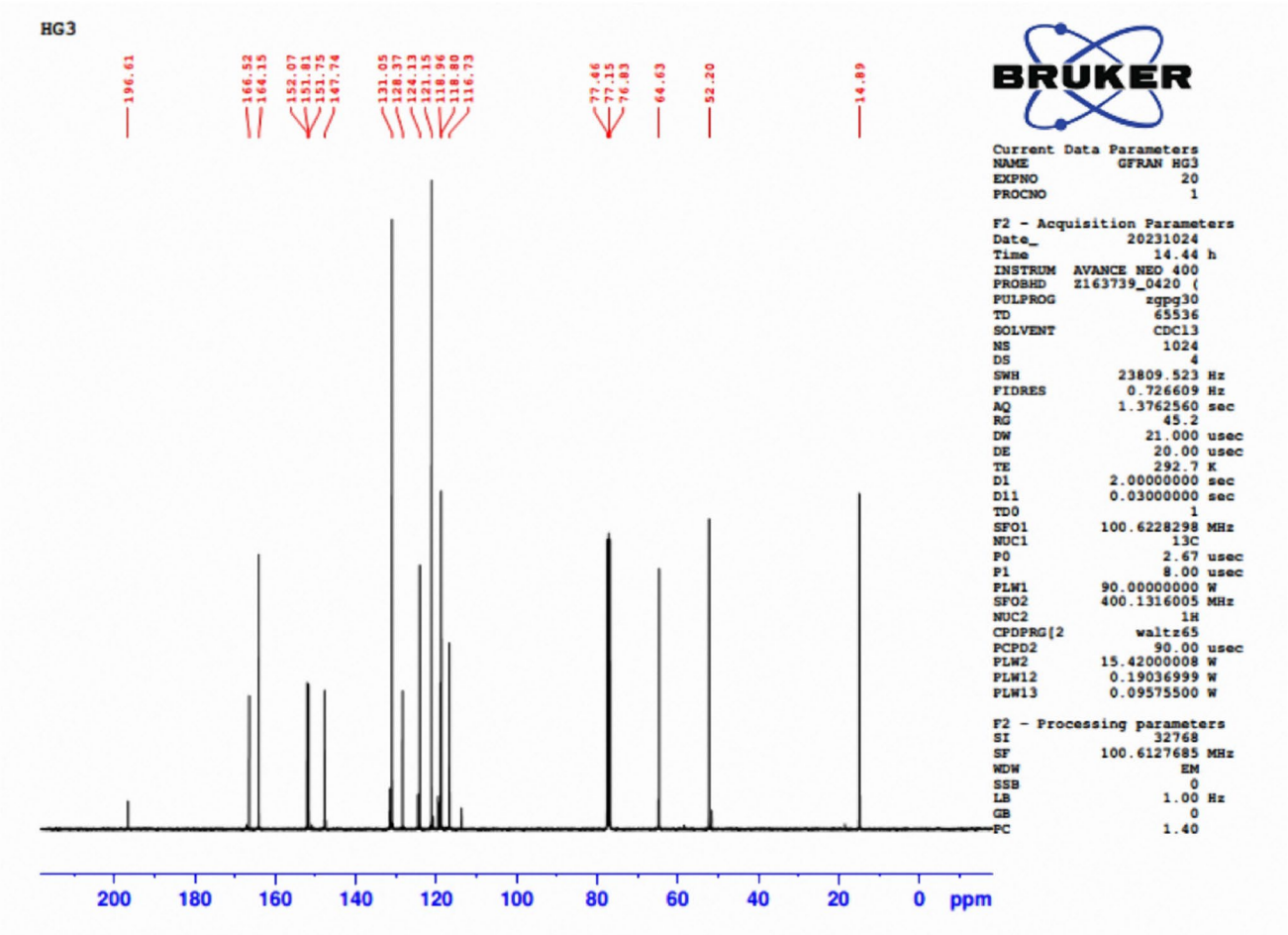

Fig. 6 ^{13}CNMR spectrum of the LS2 compound

1570 and 1442 cm^{-1}, as shown in Table 1 and Fig. 3. The molecular ion peaks were observed in the mass spectra of the compound at m/z = 299.1, with an 85% abundance, which corresponds to [C17H17NO4] + . Additionally, base peaks were observed at m/z = 284.1, as illustrated in Fig. 4. And the characteristic chemical shift ($CDCl_3$ as a solvent) was illustrated in Fig. 5. The ^{1}H NMR spectrum of the LS2 compound exhibited a singlet at 13.36 ppm, corresponding to the proton of the OH group, and a singlet at 8.62 ppm, corresponding to the azomethine proton (CH = N). The aromatic protons facilitated the observation of several signals within the range of 8.09–6.84 ppm. In the $CDCl_3$ solvent, the ^{13}C NMR spectrum of LS2 compounds, illustrated in Fig. 6, displayed a chemical shift at 164.15 ppm corresponding to the carbon atom of the (CH = N) group and a chemical shift at 152.07 ppm associated with the carbon atom of the (C–OH) group. The chemical shift in the 131.05–116.73 ppm range is ascribed to the aromatic carbons [26, 27].

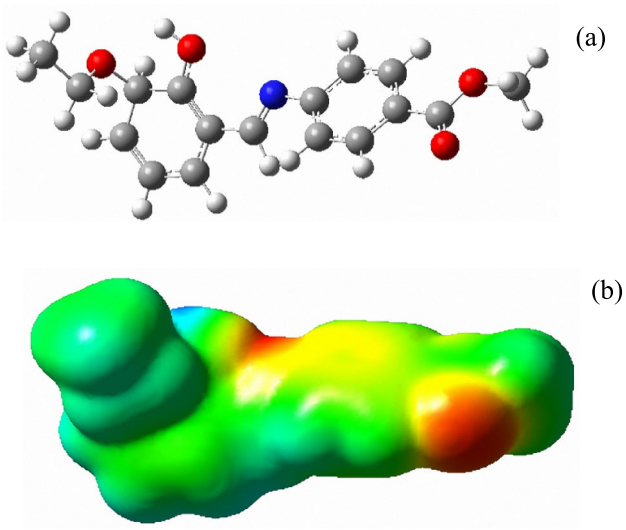

Fig. 7 **a** Optimized model (**b**) molecular electrostatic potential (MEP) surface

Analysis of the Electronic Structure Dipole Moment, Polarizability, Hyperpolarizability, and Nonlinear Optical (NLO) Properties

In the program Gaussian 09 [28], the molecular electrostatic potential (MEP) surface of the optimized model is shown in Fig. 7. One of the most important quantities in chemistry is the dipole moment of the molecule. The estimation of infrared spectrum and the long-range interactions between electrostatics and induction is crucial [29]. When the centers of positive and negative charges in a molecule are apart, an electric dipole is created. This polarity was named by scientists [30]. Its linear polarizability (α') explains the first-order response of the dipole moment to external electric fields [31]. Linear optical properties such as absorption and refractive indices are altered by changes in polarizability [32]. The tendency of a molecule to form a dipole in the presence of an electric field is measured by its hyperpolarizability (β). Thus, hyperpolarizability can be used to measure changes in the charge distribution of an atom or molecule caused by an electromagnetic field [33]. Hyperpolarizability is a sign of extensive intramolecular charge transfer (ICT) in compounds, indicating a NLO response [34]. Nonlinear changes in absorption or refractive index are examples of the NLO response caused by the interaction of quasi-delocalized electrons with applied electric fields [35]. The calculated values for dipole moment (μ), polarizability (α'), and hyperpolarizability (β) are listed in Table 2 The physical properties of the LS2 compound were compared with urea, PNA, urea-sulfamic acid, and 2M4NA as a standard material [36–40]. Compared to urea sulfonic acid, the LS2 molecule has a lower dipole moment value. Conversely, the α' and β values of urea-sulphamic acid are greater than those of the LS2 molecule. On the other hand, urea-sulphamic acid has lower values of α' and β than the LS2 molecule. The results of the

Table 2 With different reference GCRD values, the basis set 6–311 + G(d,p) was used to calculate the LS2 connection at DFT/B3LYB

Chemical quantum descriptors	LS2 compound	Urea[13]	Urea- sulphamic acid[14]	PNA[15]	2M4NA[16]
HOMO (eV)	−5.133	−7.379	−8.092	−6.639	−6.527
LUMO (eV)	−2.107	−0.362	−0.611	−2.474	−2.414
Egap (eV) = (ELUMO- EHOMO) (eV)	3.025	7.016	7.480	4.164	4.113
Dipole Moment (μ)	3.645	3.8852	4.7512	7.479	7.649
Polarizability α' (a.u)	257.386	33.802	74.406	101.802	114.595
HyperPolarizability (β)	1513.902	71.518	64.751	1660.832	1664.702

PNA P-nitroanline, *2M4NA* 2-methyl-4-nitroanline, *USA* Urea sulphamic acid

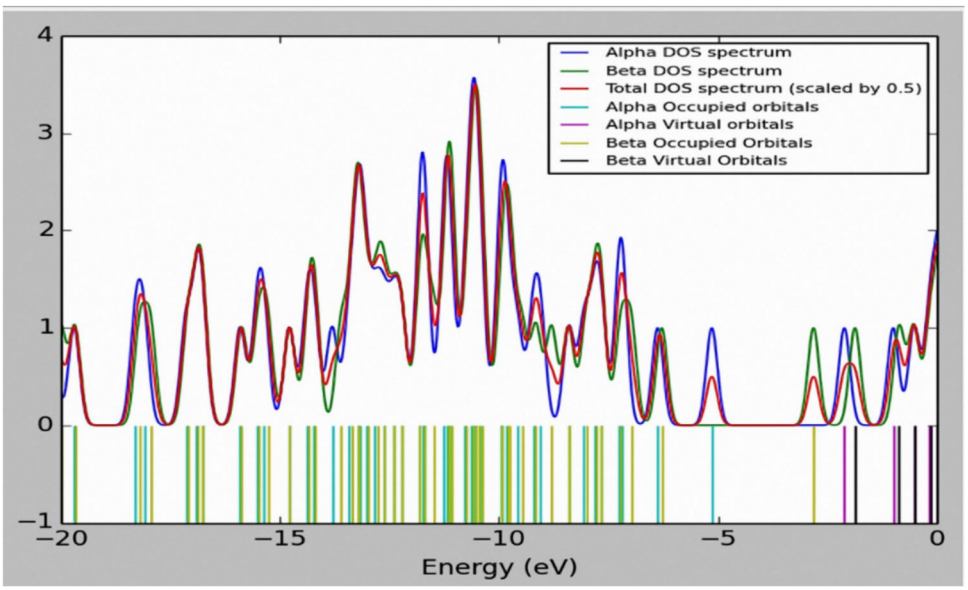

Fig. 8 The calculated DOS graph for LS2 molecule at B3LYP/ 6–311G + (d,p) level

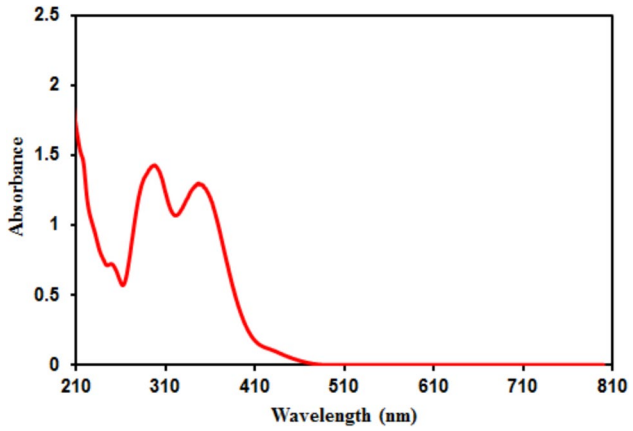

Fig. 9 The experimental UV–vis. absorption spectrum of the investigated Schiff base LS2 compound

general study suggest that the studied substance LS2 has polarizable properties.

Density of States (DOS) of Compounds

The GussSum software [41] found the density of the LS2 molecule's state spectrum. This is shown in Fig. 8. The LUMO and HOMO molecular orbits are changed by interactions, which has been shown. The amount of orbitals that can be seen at a certain energy level is shown on the DOS diagram [42].

Studies on LS2 Compound Spectroscopy

We investigated the electronic absorption of LS2 compound in an ethanol solution at a concentration of 1×10^{-4} mol L^{-1}.

Table 3 The excited states of LS2 compound, DFT/B3LYP/6-311G + (d,p)

No	Wavelength (nm)	Excitation energy (cm^{-1})	Osc. Strength	Major MO contributions (%)
1	611.6291	16,349.7777	0.0071	HOMO(A)- > LUMO(A) (74%), HOMO(B)- > LUMO(B) (11%) HOMO(A)- > L + 1(A) (5%), H-1(B)- > LUMO(B) (7%)
2	453.7857	22,036.8323	0.0076	H-1(A)- > LUMO(A) (23%), HOMO(B)- > LUMO(B) (41%), HOMO(B)- > L + 1(B) (17%), HOMO(A)- > LUMO(A) (7%), H-1(B)- > LUMO(B) (4%)
3	436.6225	22,903.0777	0.0157	H-1(A)- > LUMO(A) (31%), HOMO(A)- > LUMO(A) (12%), HOMO(B)- > LUMO(B) (30%), HOMO(B)- > L + 1(B) (19%) H-1(B)- > LUMO(B)
4	384.1466	26,031.724	0.0024	H-1(B)- > LUMO(B) (65%), HOMO(B)- > LUMO(B) (16%) HOMO(A)- > LUMO(A) (3%), HOMO(A)- > L + 1(A) (6%)
5	361.0989	27,693.2376	0.0522	H-3(A)- > LUMO(A) (19%), H-2(A)- > LUMO(A) (16%), HOMO(A)- > L + 1(A) (14%), H-1(B)- > L + 1(B) (18%) H-3(A)- > L + 1(A) (2%), H-1(A)- > LUMO(A) (4%), HOMO(A)- > LUMO(A) (4%), H-1(B)- > L + 2(B) (3%), HOMO(B)- > L + 1(B) (7%), HOMO(B)- > L + 2(B) (3%)
6	346.3511	28,872.4283	0.0284	H-1(A)- > LUMO(A) (11%), H-1(A)- > L + 1(A) (11%), HOMO(A)- > L + 1(A) (37%), HOMO(B)- > L + 1(B) (11%) H-6(A)- > LUMO(A) (2%), H-5(A)- > LUMO(A) (6%), H-1(B)- > LUMO(B) (7%), HOMO(B)- > L + 2(B) (4%)

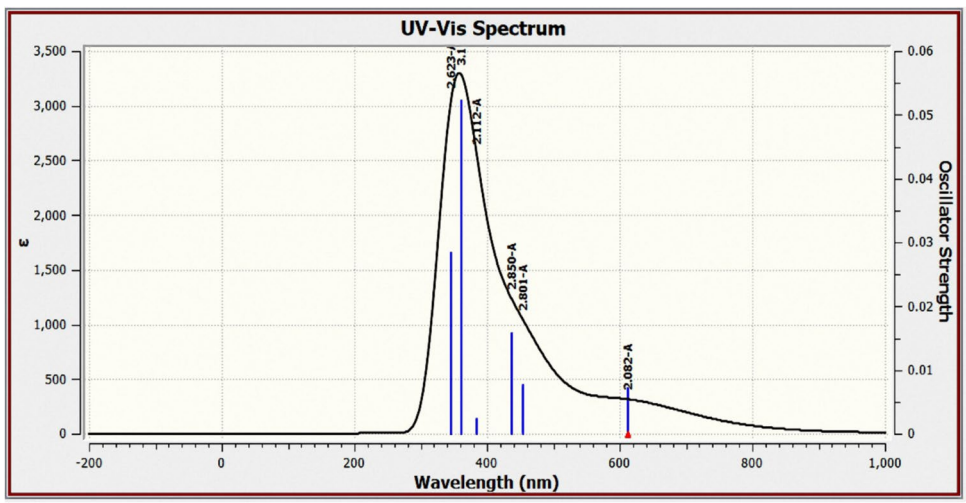

Fig. 10 Theoretical spectra calculated by TD-DFT/B3LYP/6–311 + G (d,p) of compound LS2

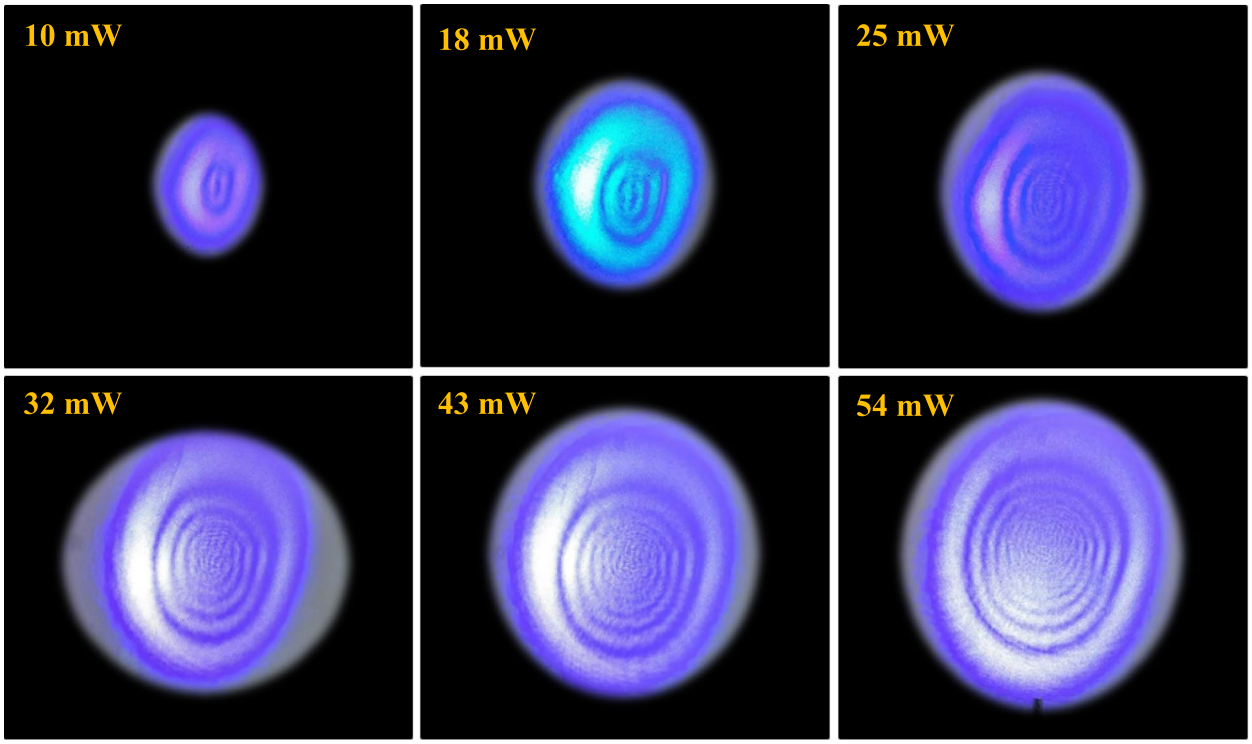

Fig. 11 Variation of DPs in LS2 compound

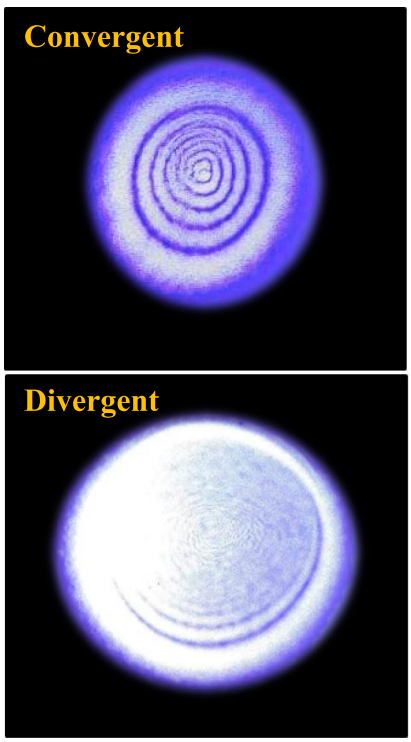

Fig. 12 Variation of DPs in LS2 compound at power input 52 mW

The wavelengths of the absorption band are 220 and 292 nm. The molar extinction coefficient is increased to 14,000 L mol^{-1}. cm^{-1}. We attribute the absorption band (CH = N) and (C = O) $\pi \rightarrow \pi^*$ transitions. The absorption spectrum of LS2 compound is displayed in Fig. 9. The linear absorption coefficient, α, of the LS2 compound at wavelengths 473 nm and 532 nm were calculated using the equation mentioned in a previous study [12] and were found to be equal to 0.25 cm^{-1} and 0.023 cm^{-1}, respectively. The electronic transitions of the LS2 compound structure are calculated using the TD-DFT/B3LYP/6-311G + (d,p) level, as shown in the UV–vis. spectrum Table 3, and Fig. 10. Calculations shows that there are six possible excited state configurations for single-electron excitations. The formation of the absorption band is primarily the result of excitation. Examination of the theoretical and experimental absorption spectra shows that the calculations were performed when the material was in the gas phase, which may have resulted in an overestimation of the vertical transition energy [43].

Nonlinear Study

DPs Experiment

Figures 11, 12, and 13 shows the far-field DPs as the laser beam's power is slowly increased, along with the effect of the beam wave front and its temporal evolution. In Fig. 11

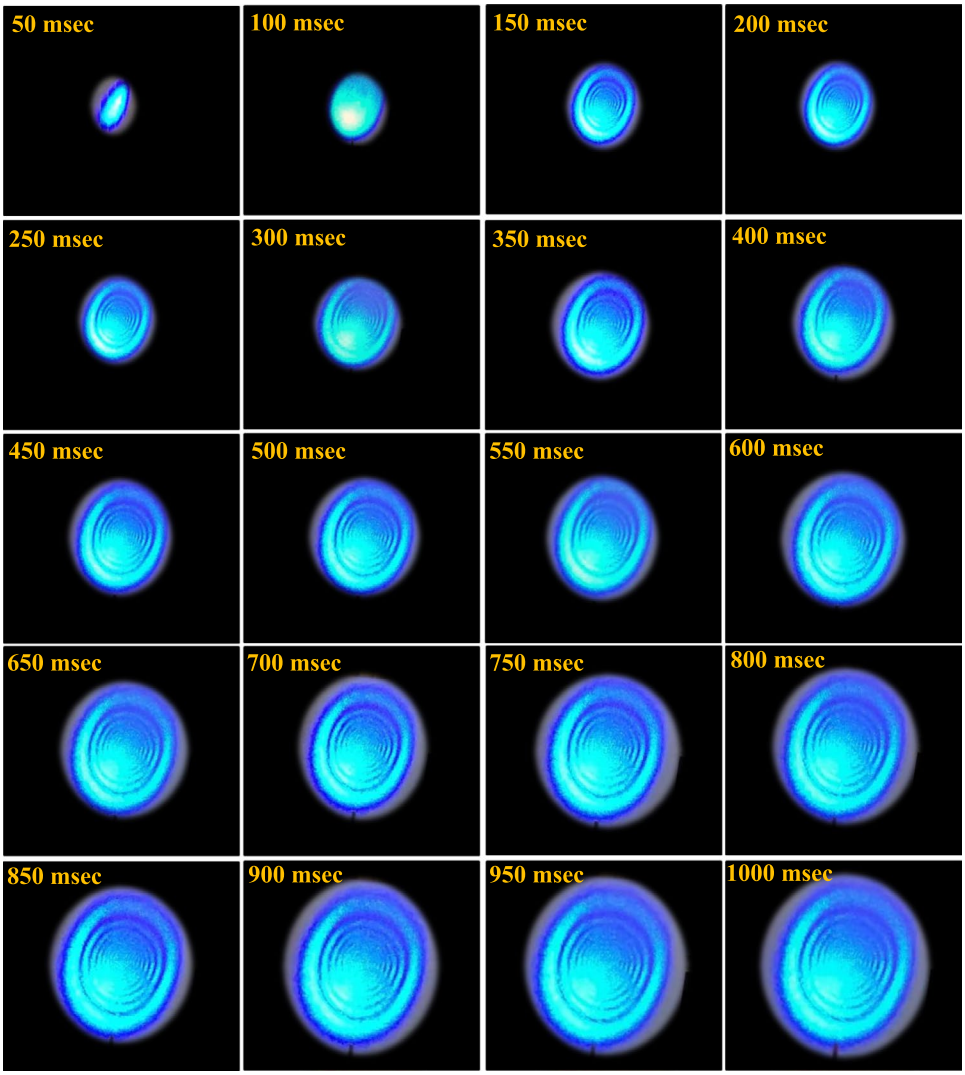

Fig. 13 Temporal evolution of a DP in LS2 compound at input of 52 mW

the DPs seen on the screen evolve with power input from single spot of small size that increases with input power an indication of the growing self-defocusing (SDF) that breaks at a certain power input to DP whose number increases with power input, then an asymmetry appeared in the upper half of the DPs, an effect seen the last 5 years extensively due to the thermal convection current [44]. The effect of beam wave front, an effect noticed as early as 1984 by Santanato and Shen [45], Deng et al. [46] and Chavez –Cerda [47], as shown in Fig. 12. The temporal behavior of the DPs is shown in Fig. 13 where the evolution follows the same trend of that seen in Fig. 11.

AOS Experiment

In these experiments, a technique known as the all-optical switching is demonstrated where a beam of light controls another beam of light on the basis of cross-self-phase modulation (XSPM) [48–50]. Here a laser beam with $\lambda = 473$ nm, the controlling beam where the nonlinear medium has large absorption coefficient so that high amount of energy is absorbed by the medium from the beam so that DPs resulted easily generated since the medium temperature increase in the Gaussian distribution. The medium has a low absorption coefficient, which results in a small quantity of energy being absorbed by the medium and no DPs being produced by the other beam, which is the controlled at $\lambda = 532$ nm. The signal for the beam 532 nm is manipulated by the beam 473 nm when both beams travel through the nonlinear medium simultaneously. Two experiments were implemented. In the first case, both the controlling beam and the controlled beam are CW, which means that there is static all-optical switching. In the second one, the controlling beam is converted to a pulse by connecting the laser head to the TTL function of a frequency generator so that it

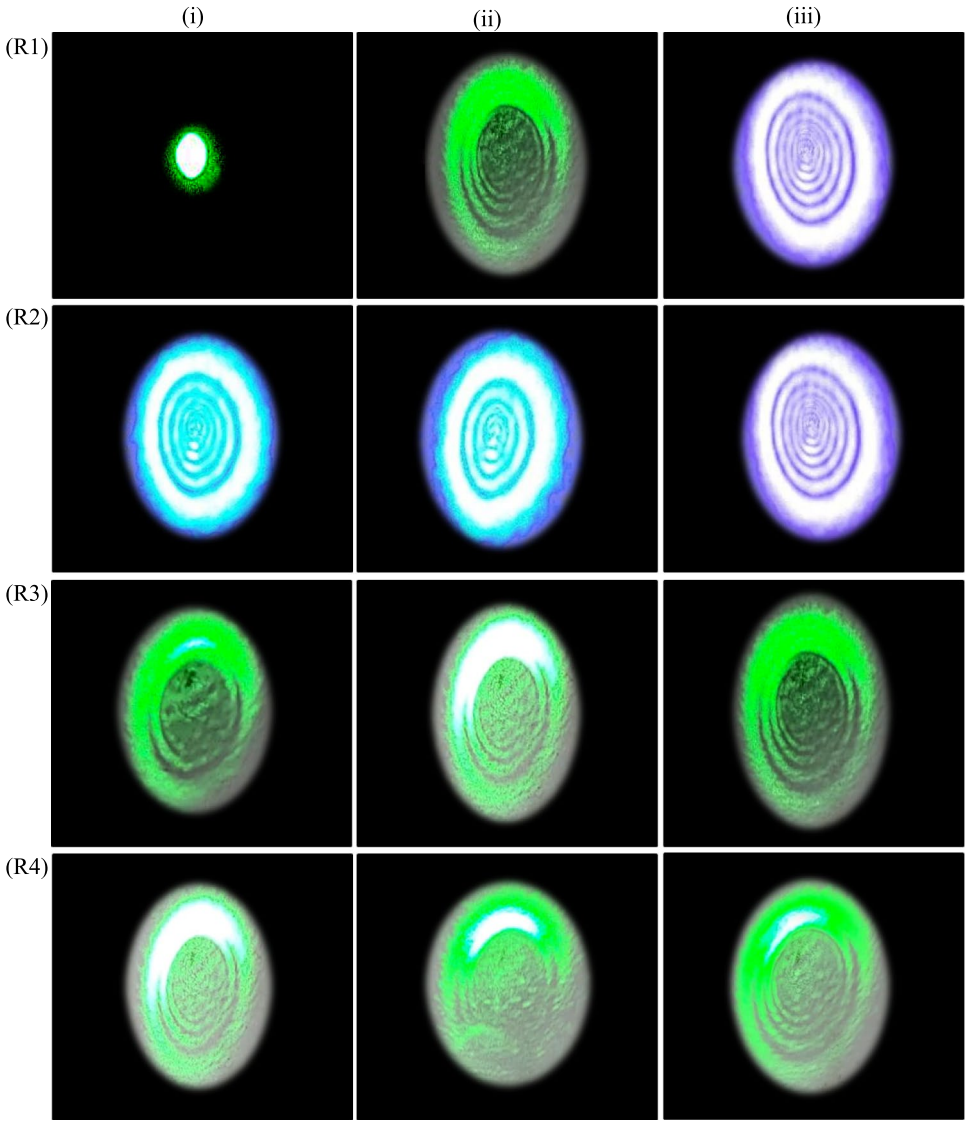

Fig. 14 Static AOS in LS2 compound

become pulsed (square) while maintaining the controlled CW beam, resulting in a pulse AOS or dynamic DPs. Figures 14 and 15 illustrate the outcomes of both investigations. In Fig. 14 R1 i single spot resulted when the controlled 532 nm beam traverse the sample. When the controlling 473 nm beam traverse the sample DPs resulted as shown in Fig. 14 R1iii and when both beams pass the sample simultaneously two DPs types resulted as shown in Fig. 14 R1ii-iii. Figure 14 R2, R3 and R4 shows the effect of the controlling beam on its DPs, the effect of the controlling on the controlled DPs and controlled beam effect on its DPs. In Fig. 15 the experiment described in Fig. 14. The controlling beam 473 nm changed to pulsed (square pulse) by connecting the laser head to the TTL function of a frequency generator, keeping the controlled 532 nm CW. The pulse signal length was 1 s so that temporal sequence of DPs belongs to the beam 473 nm followed by sequence of the 532 nm beam.

Z-Scan

We obtained a straight line when conducting open aperture (OA) Z-scan measurements as shown in Fig. 16a, which proves that the LS2 compound does not have a nonlinear absorption coefficient (NLAC). While we obtained a peak followed by a valley when curried out the closed aperture (CA) Z-scan, as can be seen in Fig. 16b, that is, the occurrence of SDF, which indicates that the LS2 compound has a negative NLRI, n_2. It should be noted here that both Z-scan measurements were performed using an input power of P = 5 mW, which corresponds to the intensity I = 860.76 W/cm^2.The origin of the nonlinearity is

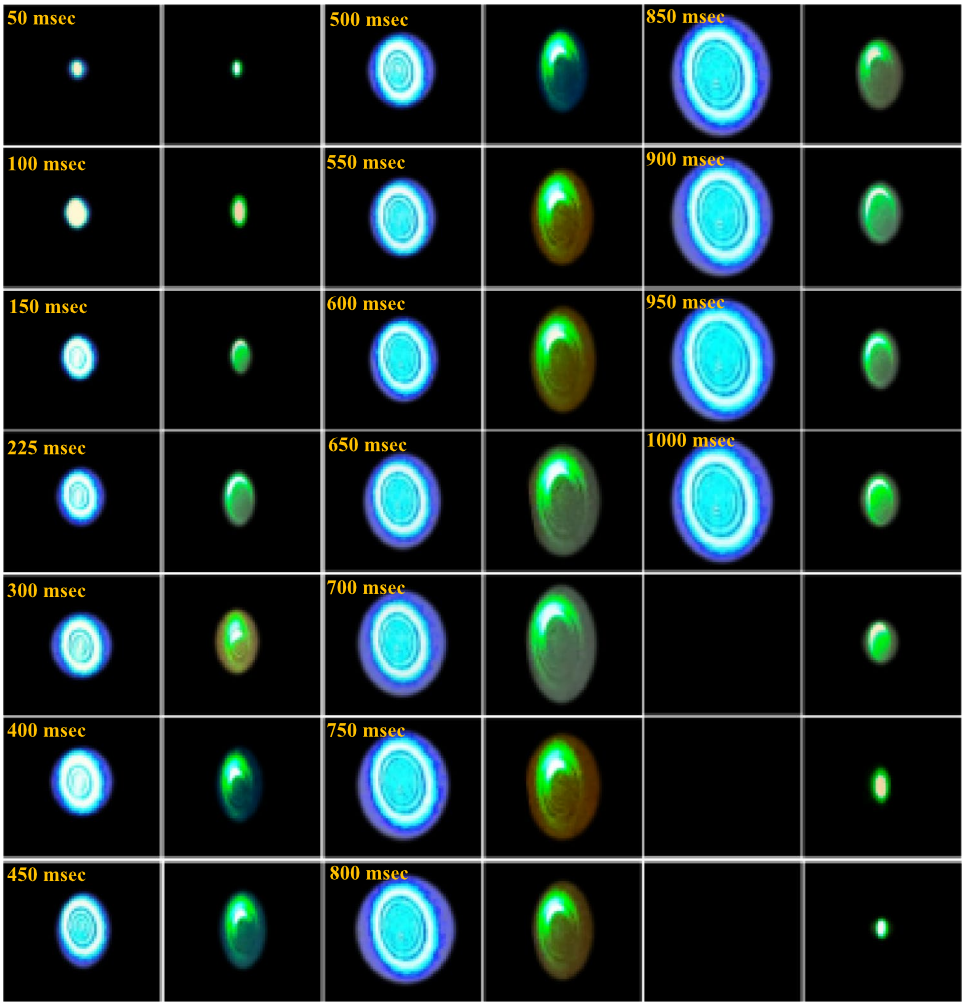

Fig. 15 Dynamic AOS in LS2 compound

thermal due to the use of a continuous wave laser beam. The Z-scan experiment was repeated several times and we found that the error rate in the measurements was less than $\pm 1\%$.

Determine the NRI, n_2 due to

DPs

Based on the results of subsection (3.5.1), the number of rings per each pattern increased with power input, P, directly, so that the medium temperature, the medium refraction index, and the beam phase all increase. Based on the medium thickness, d, beam wavelength λ, maximum number of rings, N, beam spot size, ω, and power input the NLRI, n_2, can be estimated using the following equation [51]

$$n_2 = \frac{\pi}{2}\frac{N\lambda\omega^2}{Pd} \tag{1}$$

For N=10,ω =19.235 μm, λ=473 nm, P=52 mW, beam intensity $I = \frac{2P}{\pi\omega^2}$, d =0.1 cm,I =8779.85 W/cm^2 and n_2 =5.387×10^{-7} cm^2/W.

Z-Scan

Since the nonlinearity is of thermal origin, the NLRI can be determined from the following equation [52, 53]

$$n_2 = \frac{\Delta T_{p-v}\,\lambda}{4\pi dI} \tag{2}$$

ΔT_{p-v} is the difference between the peak transmittance and valley transmittance λ=473 nm, d=0.1 cm I=860.76 W/ cm^2. The NLRI, n_2 value of the LS2 compound was determined from Eq. 2 and Fig. 16b was found equal to 0.12×10^{-7} cm^2/W.

Due to the different of the beam power used in both techniques viz. 52 mW in the DPs and 5 mW in the Z-scan it is expected that two n_2 values resulted, due to the DPs

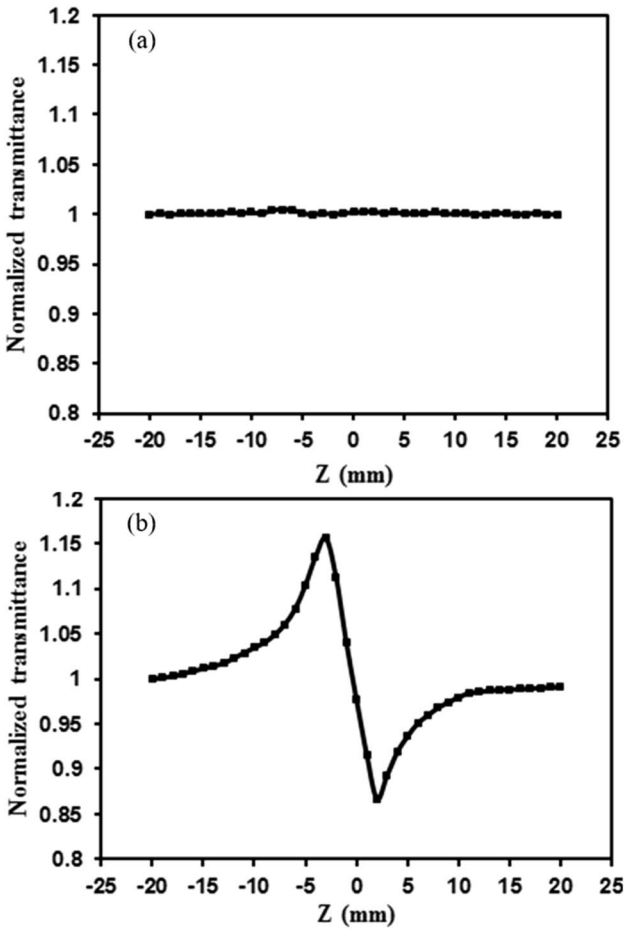

Fig. 16 **a** OA Z-scan in LS2 compound **b** CA Z-scan in LS2 compound at input power at 5 mW

technique is larger than the Z-scan. We find that the value of the NLRI of the LS2 compound is greater than that of materials known to possess high values of the NLRI, such as those mentioned in studies [54–58], when compared to them. Which proves that the LS2 compound prepared in the current work can be a candidate for use in optical devices.

Conclusion

The passage of a low-power, cw laser beam through the Schiff base compound led to the formation of multiple diffraction patterns (DPs). Self-defocusing phenomenon was observed, which resulted in a thermal effect in the Schiff base compound. A nonlinear refractive index (NLRI) of 5.387×10^{-7} cm^2/W was determined by the number of rings at the high-power input. The NLRI was also calculated using a close aperture Z-scan. Using laser beams with wavelengths of 473 nm and 532 nm, the all-optical switching phenomenon was demonstrated. The purpose of the present work was accomplished by finding a material with high optical properties.

Authors' Contributions "Ghufran A. Mirdan and Mouayed Y. Kadhum synthesis the compound, Qusay M.A. Hassan and C. A. Emshary wrote the main manuscript text – review and editing, Kawkab Ali Hussein and H. A. Sultan participated in the characterization and analysis of the results, Sadiq M. H. Ismael and Hasanain A Abdullmajed taking measurements."

Data Availability No datasets were generated or analysed during the current study.

Declarations

Ethics Approval and Consent to Participate The authors declare that their commitment to ethics related to his work and they have designed the experiments, collected and analyzed the data, and written the manuscript.

Consent for Publication The authors declare their consent of publication.

Competing Interests The authors declare no competing interests.

References

1. Jassem AM, Hassan QM, Emshary CA, Sultan HA, Almashal FA, Radhi WA (2021) Synthesis and optical nonlinear properties performance of azonaphthol dye. Phys Scr 96(2):025503
2. Qusay M.A. Hassan, H.A. Sultan, Ahmed S. Al-Asadi, Ayat Jawdat Kadhim, Nazar A. Hussein, C.A. Emshary (2019) Synthesis, characterization, and study of the nonlinear optical properties of two new organic compounds, Synth. Mat. 257 :116158(14 pp).
3. Kawkab Ali Hussein, H. A. Sultan, Afrah Abdul-Radha, Mahdi Aljaber, Qusay M. A. Hassan, C. A. Emshary (2024) Synthesis, h.characterization and nonlinear optical properties of new azo compound using CW laser beam, Opt. Quan. Electron. 56:1056(20 pp)
4. Adil Muala Dhumad, Qusay M. A. Hassan, C.A. Emshary, Tarek Fahad, Nabeel A. Raheem, H.A. Sultan (2021) Nonlinear optical properties investigation of a newly synthesised Azo-(β)- diketone dye, J. Photochem. Photobiol., A: Chem. 418 :113429 (17 pp).
5. Uhood J. Al-Hamdani, Qusay M.A. Hassan, Ahmed M. Zaidan, H.A. Sultan, Kawkab Ali Hussain, C.A. Emshary , Zainab T.Y. Alabdullah (2022) Optical nonlinear properties and all optical switching in a synthesized liquid crystal, J. Molec. Liq. 361 :119676 (13 pp)
6. Qusay M. A. Hassan, C. A. Emshary, H. A. Sultan (2021) Investigating the optical nonlinear properties and limiting optical of eosin methylene blue solution using a cw laser beam, Phys. Scr. 96 :095503 (16 pp).
7. Sana K. Khalaf , Qusay M.A. Hassan, C.A. Emshary , H.A. Sultan (2022) Concentration effect on optical properties and optical limiting of PVA doped with nigrosin films, J. Photoch. Photo., A: Chem. 427 :113809 (11 pp).
8. D. Z. Mutlaq, Qusay M. A. Hassan, H. A. Sultan, and C. A. Emshary (2020) The optical nonlinear properties of a new

synthesized azo-nitrone compound, Opt. Mater., 113:110815 (15 pp)
9. Hassan Naeem Hasnawi, Kawther Saleh Thanon, Qusay M.A. Hassan, Adil Muala Dhumad a, H.A. Sultan b, C.A. Emshary (2024) Synthesis, DFT, molecular docking and optical nonlinear studies of a new phthalimide derivative, J. Molec. Liq. 400 :124437 (12 pp)
10. Sultan HA, Hassan QMA, Al-Asadi AS, Elias RS, Bakr H, Saeed BA, Emshary CA (2018) Far-field diffraction patterns and optical limiting properties of bisdemethoxycurcumin solution under CW laser illumination. Opt Mater 85:500–509
11. Al-Asadi AS, Hassan QMA, Abdulkader AF, Mohammed MH, Bakr H, Emshary CA (2019) Formation of graphene nanosheets/ epoxy resin composite and study its structural, morphological and nonlinear optical properties. Opt Mater 89:460–467
12. Uhood J. Al-Hamdani, Qusay M.A. Hassan, C.A. Emshary, H.A. Sultan, Adil Muala Dhumad, Afrah A. Al-Jaber (2021) All optical switching and the optical nonlinear properties of 4-(benzothiazolyldiazenyl)-3-chlorophenyl 4-(nonylthio)benzoate (EB-3Cl), Optik 248 :168196 (17 pp).
13. Gordon JP, Leite RC, Moore RS, Porto SPS, Whinner JR (1965) Long-transient effect: in lasers with inserted liquid samples. J Appl Phys 36:3–8
14. Durbin SD, Arakelian SM, Shen YR (1981) Laser- induced diffraction rings from a nematic – liquid- crystal film. Opt Lett 6:411–413
15. Sheik-Bahae M, Said AA, Van Stryland EW (1989) High sensitivity single beam n_2 measurements. Opt Lett 14:955–957
16. Sheik-Bahae M, Said AA, Wei T, Hagan DJ, Van Stryland EW (1990) Sensitive measurement of optical nonlinearities using a single beam, IEEE. J Quant Electron 26:760–769
17. Brodowska K, Lodyga-archruscinska E (2011) Schiff base interesting range of applications in an various fields of sciences. Sci Tech 68:132–134
18. Wang L, Hao S, Zhang W, Liu Y, Yu G (2013) Synthesis, structural, optoelectronic properties of novel zine Shiff base complexes, Chi. Sci, Bull 58:2733–2740
19. Mahdi BS (2022) Preparation and investigated third-order optical nonlinearities of Schiff bases by using the Z-scan. Neuroquantology 20:28–33
20. L. Rigamonti (2010) Schiff base metal complexes for second order nonlinear optics, La Chim. I'Industria, 3:118(5 pp).
21. Almashal FA, Mohammed MQ, Hassan QMA, Emshary CA, Sultan HA, Dhumad AM (2020) Spectroscopic and thermal nonlinearity study of a schiff base compound. Opt Mater 100:109703
22. Ahmed Majeed Jassem, Qusay M.A. Hassan, Faeza Abdulkareem Almashal, H.A. Sultan, Adil Muala Dhumad, C.A. Emshary, Luma Taher Tuma Albaaj (2021) Spectroscopic study, theoretical calculations, and optical nonlinear properties of amino acid (glycine)-4-nitro benzaldeyhyde-derived Schiff base, Optical Materials 122 :111750 (17 pp).
23. Hasanain A. Abdullmajed, H. A. Sultan, Rafid H. Al-Asadi, Qusay M. A. Hassan , Asaad A. Ali ,C. A. Emshary (2022) Synthesis, DFT calculations and optical nonlinear properties of two derived Schiff base compounds from ethyl-4-amino benzoate, Phys. Scr. 97 :025809 (18 pp)
24. Jinan Khudhair Salim, Qusay M.A. Hassan, Ahmed Majeed Jassem, H.A. Sultan, Adil Muala Dhumad, C.A. Emshary (2022) An efficient ultrasound-assisted CH3COONa catalyzed synthesis of thiazolidinone molecule: Theoretical and nonlinear optical evaluations of thiazolidinone-Schiff base derivative, Optical Materials 133 :112917(13 pp)
25. Zahraa Salman Fadhil, Qusay M. A. Hassan, Kawkab Ali Hussein, H. A. Sultan, Jasim M. S. Al Shawi. C. A. Emshary (2024) Studies of the nonlinear optical properties of a synthesized Schiff base ligand using visible cw laser beams, Phys. Scr. 99 :065525(18 pp).
26. Donald L. Pavia, Gary M. Lampman, George S. Kriz., Introduction to spectroscopy, A Guide for Students of Organic Chemistry, Bellingham, Washington, USA, third edition, 2001.
27. Robert M. Silverstein., Francis X. Webster., Spectrometric Identification of Organic Compounds., Sixth Edition., John Wiley & Sons, Inc., New York., 1997.
28. Gaussian 16, Revision C.01, M. J. Frisch, G. W. Trucks, H. B. Schlegel, G. E. Scuseria, M. A. Robb, J. R. Cheeseman, G. Scalmani, V. Barone,G. A. Petersson, H. Nakatsuji, X. Li, M. Caricato, A. V. Marenich, J. Bloino, B. G. Janesko, R. Gomperts, B. Mennucci, H. P. Hratchian, J. V.Ortiz, A. F. Izmaylov, J. L. Sonnenberg, D. Williams-Young, F. Ding, F. Lipparini, F. Egidi, J. Goings, B. Peng, A. Petrone, T. Henderson, D.Ranasinghe, V. G. Zakrzewski, J. Gao, N. Rega, G. Zheng, W. Liang, M. Hada, M. Ehara, K. Toyota, R. Fukuda, J. Hasegawa, M. Ishida, T.Nakajima, Y. Honda, O. Kitao, H. Nakai, T. Vreven, K. Throssell, J. A. Montgomery, Jr., J. E. Peralta, F. Ogliaro, M. J. Bearpark, J. J. Heyd, E. N. Brothers, K. N. Kudin, V. N. Staroverov, T. A. Keith, R. Kobayashi, J. Normand, K. Raghavachari, A. P. Rendell, J. C. Burant, S. S. Iyengar, J. Tomasi, M. Cossi, J. M. Millam, M. Klene, C. Adamo, R. Cammi, J. W. Ochterski, R. L. Martin, K. Morokuma, O. Farkas, J. B. Foresman, and D. J. Fox, Gaussian, Inc., Wallingford CT, 2016.
29. M. Veit, , D. M. Wilkins, Y. Yang, R. A. DiStasio, M. Ceriotti (2020) Predicting molecular dipole moments by combining atomic partial charges and atomic dipoles. J. of Chem. Phys.153 :04113(14 pp).
30. Moldoveanu S, David V (2013) Essentials in modern HPLC separations. Elsevier, Amsterdam, Netherlands
31. Sabin JR, Zerner MC, Brändas E, Hanstrop D (1998) Advances in Quantum Chemistry. Academic Press, San Diego
32. Sekkat Z, Knoll W (2002) Photoreactive Organic Thin Films. Academic Press, Amsterdam
33. Vivas MG, Silva DL, Rodriguez RD, Canuto S, Malinge J, Ishow E, De Boni L (2015) Interpreting the first-order electronic hyperpolarizability for a series of octupolar push-pull triarylamine molecules containing trifluoromethyl. The Journal of Phys Chem C 119:12589–12597
34. Khan MU, Ibrahim M, Khalid M, Braga AAC, Ahmed S, Sultan A (2019) Prediction of second-order nonlinear optical properties of D–π–A compounds containing novel fluorene derivatives: A promising route to giant hyperpolarizabilities. J Cluster Sci 30:415–430
35. S. Kobayashi, K. Müllen, (Eds.). (2015). Encyclopedia of polymeric nanomaterials. Berlin Heidelberg: Springer Berlin Heidelberg.
36. Migalska-Zalas A, El Korchi K, Chtouki T (2018) Enhanced nonlinear optical properties due to electronic delocalization in conjugated benzodifuran derivatives. Opt Quant Electron 50:1–10
37. Urea Hamdan A. S. Al-Shamiri, Mahmoud E. M. Sakr, Samir A. Abdel-Latif, Nabel A. Negm, Maram T. H. Abou Kana, Samy A. El-Daly, Ahmed H. M. Elwahy (2022) Experimental and theoretical studies of linear and non-linear optical properties of novel fused-triazine derivatives for advanced technological applications., Sci. Rep. 12 :19937.
38. Senthilvelan N, Rajarajan G, Jegatheesan A, Sivakumar S, Elanchezhiyan J (2017) Growth and Spectroscopic Characterization of urea Sulphamic acid crystal: A second-order nonlinear material. Rasayan J Chem 10:218–225
39. Shimaa Abdel Halim (2018) TD-DFT calculations, electronic structure, natural bond orbital analysis, nonlinear optical properties electronic absorption spectra and antimicrobial activity

application of new bis-spiropipridinon/pyrazole derivatives. Eur J Chem 9:287–302
40. Lópeza SF, Mezaa MP, Hoyos FT (2018) Study of the nonlinear optical properties of 4-nitroaniline type compounds by density functional theory calculations: Towards new NLO materials. Comput Theor Chem 1133:25–32
41. O'boyle NM, Tenderholt AL, Langner KM, (2008) Software news and updates cclib: A library for package-independent computational chemistry algorithms. J Comput Chem 29:839–845
42. Rouhani M (2019) A detailed computational investigation on the structural and spectroscopic properties of propolisbenzofuran B. Heliyon 5:e02518
43. H.A. Sultan, Adil Muala Dhumad, Qusay M.A. Hassan, Tarek Fahad, C.A. Emshary , Nabeel A. Raheem (2021) Synthesis, characterization and the nonlinear optical properties of newly synthesized 4-((1,3-dioxo-1-phenylbutan-2-yl)diazenyl) benzenesulfonamide, Spectrochimica Acta Part A: Molecular and Biomolecular Spectroscopy 251 :119487(15 pp).
44. Qusay M.A. Hassan, Nabeel A. Raheem, C.A. Emshary, Adil Muala Dhumad , H.A. Sultan, Tarek Fahad (2022) Preparation, DFT and optical nonlinear studies of a novel azo-(β)- diketone dye, Opt. Las. Technol. 148 :107705(14 pp).
45. Santamato E, Shen YR (1984) Field curvature effect on the diffraction ring pattern of laser beam dressed by spatial self-phase modulation in animatic film. Opt Lett 9:564–566
46. Deng L, He K, Zhou T, Li C (2005) Formation and evolution by Far-filed diffraction patterns of divregean and convergant Gaussian beam passing through self-focusing and self-defocusing media, J. Opt A: Pure Appl 7:409–415
47. S. Chavez –Cerda, C. M. Nascimento, M. A. R. C. Alencar, M. G. A. da silva, M. R. Mene ghetto, J. M. Hickman (2006) Experimental observation of the Far field diffraction pattern of diveregent and convergent Gaussian beam in a self-defocusing medium, Annals of Optics XXIX:1–4.
48. Jia Y, Shan Y, Wu L, Dai X, Fan D, Xiang Y (2018) Broadband nonlinear optical resonance and all-optical switching of liquid phase exfoliated tungsten diselenide. Photo Res 5:1040–1047
49. Q. Wang, X. Wu, L. Wu, Y. Xiang (2019) Broadband nonlinear optical response in Bi2Se2-Bi2Te3 heterostructure and its application in all-optical switching, AIP Adv. 9 :025022 (7 pp).
50. Zhang XJ, Yuan ZH, Yang RX, He Y, Qin YL, Si X, Jun H (2019) A review on spatial self-phase modulation of two-dimensional material. J Cent South Univ 26:2295–2306
51. Ogusu K, Kohtani Y, Shao H (1993) Laser- induced diffraction rings from an absorbing solution. Opt Rev 3:232–234
52. Cuppo FLS, Neto AMF, S. L. G´omez and P. Palffy-Muhoray, (2002) Thermal-lens model compared with the Sheik-Bahae formalism in interpreting Z-scan experiments on lyotropic liquid crystals. J Opt Soc Am B 19:1342–1348
53. Sendhil K, C. Vijayan_and M.P. Kothiyal, (2006) Low-threshold optical power limiting of cw laser illumination based on nonlinear refraction in zinc tetraphenyl porphyrin. Opt Las Technol 38:512–515
54. Parvin M, Ahmud B (2014) Investigation of optical limiting properties of azophloxine dye using nanosecond z-scan technique. Int J chem Tech Res 6:2493–2498
55. Duskova E, Pshenychni A, sauchez-Ferrer A, Lysenko D, Vaqaavuori J, Kaivola M, (2014) Enhanced nonlinearity by H. bonded polymer-dye complex in liquid crystal for holographic gratings. J Opt Am 31:1456–1464
56. Chaulia s n, (2016) Synthesis, spectral, computational and biological study of Co (II), Ni (II), Cu (II) and Zn (Ii) complexes with azo derived from 4, 4-diaminodiphenyl sulphone and 5-sulphosalicylic acid. J Chem Pharma Res 8:242–258
57. Albasha M (2018) Synthesis, Characterization of new azo compounds and their biological evaluation, int. J Acad Sci Res 6:16–24
58. Ben khaya S, Mrabet S, Eltlarfi A (2020) Classifications, properties, recent synthesis and application of azo dyes, tleliyon 6: e03271 .